Analyst

Accepted Manuscript

This article can be cited before page numbers have been issued, to do this please use: Z. Hu, R. Xu, S. Yu, J. Li and Z. Yang, *Analyst*, 2020, DOI: 10.1039/D0AN01553A.




ROYAL SOCIETY OF CHEMISTRY

rsc.li/analyst

View Article Online
DOI: 10.1039/D0AN01553A

ARTICLE

# Facile synthesis of nanorod-like $MoS_2$ nanostructure for sensitive electrochemical biosensing application

Received 00th January 20xx,
Accepted 00th January 20xx

DOI: 10.1039/x0xx00000x

Zhongfang Hu,[a] Rong Xu,[a] Suhua Yu,[b] Juan Li, [a,*] Zhanjun Yang[a,b]

A novel nanorod-like $MoS_2$ semiconductor nanostructure was synthesized through a simple two-step method. Nanorod-like $MoS_2$ nanostructure was exploited as electrode material to immobilized enzyme and electrochemical sensing application. Characterizations of nanorod-like $MoS_2$ nanostructure and the resultant biosensor were performed by scanning electron microscope, Fourier transform infrared spectroscopy, electrochemical impedance spectrum, and cyclic voltammetry. Enzyme molecules loaded at $MoS_2$ nanostructure retained their native structure and bioactivity. The direct electron transfer of glucose oxidase at $MoS_2$ nanostructure coated glassy carbon electrode was enhanced greatly. At an optimal potential of -0.45 V, the electrochemical glucose sensor had wide linear ranges of $1.5\times10^{-5}$-$3.25\times10^{-4}$ M and $3.25\times10^{-4}$-$1.43\times10^{-3}$ M, and a low detection limit of 0.005 mM (S/N = 3) with a high sensitivity of 25.06 ± 0.5 mA $M^{-1}$ $cm^{-2}$. At the same time, the present biosensor showed excellent selectivity, reproducibility and stability for glucose. What's more, the biosensor was successfully applied to determination of practical samples.

## Introduction

Effective measurement of glucose in the blood is of crucial importance to diagnose and treat diabetes patients[1,2]. Electrochemical biosensors are widely used in glucose detection because of their simple equipment, high detection sensitivity, fast assay speed, excellent selectivity, and easy operation[3-5]. Owing to strong catalytic oxidization capacity to glucose molecules, glucose oxidase (GOx) has been extensively explored to develop electrochemical sensors for the determination of glucose[6,7]. More and more researchers have been working on the design of third-generation biosensors, which is based on direct electron transfer (DET) of redox-active center of GOx trapped on the modified electrode[8,9]. Nevertheless, the redox center of the enzyme is deeply embedded in the enzyme shell, which creates a barrier to the DET process between the redox-active of GOx and electrode surface[10,11]. In recent years, it has been found that the characteristic structure of nanomaterials can accelerate DET process[12-15]. Therefore, the modification of nanomaterials on electrodes for glucose biosensing has attracted wide attention [15-22]. Among many nanomaterials, semiconductor nanomaterials with heterogeneous structures has gained increasing interests in development of DET-based electrochemical biosensors.

The transition metal sulfide semiconductor has been widely used in sensor[23], battery[24], capacitor[25], tribology[26], catalysis[27] and other fields because of its attractive physical and chemical performances. Molybdenum disulfide ($MoS_2$) as an indirect semiconductor has a band gap of 1.29 eV, which is formed by van der Waals bonding S-Mo-S units[28-30]. The structure of S-Mo-S is similar to that of graphene[29]. In recent years, $MoS_2$ have shown great potential in electrochemical sensing fields due to layer dependent band gap, highly exposed active sites and high electron mobility. Especially, flake-shaped $MoS_2$ nanostructure have been reported as electrode materials to develop electrochemical biosensors[31-33]. Nowadays, $MoS_2$ nanoflakes were usually combined with noble metal nanoparticles to design glucose sensing[34]. For example, nanogold modified $MoS_2$ has been reported to develop a nonenzymatic electrochemical glucose biosensor[35]. However, $MoS_2$ semiconductor nanostructures have not been reported to immobilize enzyme molecules for fabrication of electrochemical glucose sensors so far. In addition, it has been proved that shape and size of nanomaterials are important factors to affect the property of the biosensors[22,35-36]. So it is very necessary to explore the synthesis of other shaped and sized $MoS_2$ materials for the biosensing application.

In this research, nanorod-like $MoS_2$ semiconductor nanostructure was synthesize using a simple one-step synthesis route. $MoS_2$ nanostructure was firstly dispersed into chitosan solution, and then used to modify electrode for the immobilization of enzyme molecules. Then a novel electrochemical biosensor was fabricated for sensitive and fast determination of glucose. Nanorod-like $MoS_2$ nanostructure has large specific surface area and obviously accelerated the DET between GOx and the modified electrode surface. The resultant electrochemical glucose biosensor showed high detection sensitivity, good selectivity and satisfactory capability for actual samples. This work provided an alternative electrode material for the fabrication of excellent biosensors.

[a] School of Chemistry and Chemical Engineering, Yangzhou University, Yangzhou 225002, PR China. Tel./Fax: +86-514-87972034. E-mail address: lijuan@yzu.edu.cn
[b] Guangling College, Yangzhou University, Yangzhou 225002, PR China.

View Article Online
DOI: 10.1039/D0AN01557A



## Experimental

### Reagents and instruments

Glucose oxidase (GOx, 108 U $mg^{-1}$, EC 1.1.3.4) produced from Aspergillus niger was bought by Amresco Chemical Co., Ltd. Chitosan and D-(+)- glucose were provided by Sigma-Aldrich (China). Ammonium molybdate tetrahydrate ($(NH_4)_6Mo_7O_{24}\cdot 4H_2O$) and sodium diethyldithiocarbamate ($(C_2H_5)_2NCS_2)_2Na\cdot 3H_2O$) were provided by Sinopharm Chemical Reagent Co., Ltd (China). The D-(+)- glucose stock solution must be placed at room temperature for 24 h to remove the optical rotation, and then used for determination. Phosphate buffer saline (PBS) was prepared by mixing 0.1 M $NaH_2PO_4$ and $Na_2HPO_4$ with a certain proportion, and the accurate pH of PBS was adjusted by a pH meter. All other chemical reagents used are of analytical grade, and their solutions were prepared with distilled water.

### Apparatus

Electrochemical measurements were conducted in a typical three-electrode cell using a CHI 852C electrochemical workstation (Shanghai Chenhua Co. Ltd, China). A conventional three-electrode system was used for all experiments, including a glassy carbon electrode (GCE, D = 3 mm) as the working electrode, a saturated calomel electrode (SCE) as reference electrode and a platinum wire as the auxiliary electrode. And pH of PBS was measured with a glass combination electrode of S-25 digital pH-meter. Morphology characterizations were performed at an acceleration voltage of 15 kV using a Hitachi S-4800 scanning electron microscope (Japan). Electrochemical impedance spectroscopy (EIS) for different electrodes was obtained in a solution of 0.10 M KCl containing 5.0 mM $K_3[Fe(CN)_6]/K_4[Fe(CN)_6]$ by an Autolab PGSTAT30 (The Netherlands). The frequency range of EIS measurement was set within a range from 0.05 to 10 kHz at a bias potential of 190 mV. A Tensor 27 spectrometer (Bruker Co., Germany) was used to measure the Fourier transform infrared (FTIR) spectrum analysis.

### Live Subject Statement

All experiments were performed in accordance with the Guidelines of China, and approved by the ethics committee at Yangzhou University. Informed consents were obtained from human participants of this study.

### Synthesis of nanorod-like $MoS_2$ semiconductor nanostructure

Firstly, $(NH_4)_6Mo_7O_{24}\cdot 4H_2O$ (4 mM) and $(C_2H_5)_2NCS_2)_2Na\cdot 3H_2O$ (20 mM) were dissolved in distilled water (400 mL) under stirring for 6 h. Then the above-mentioned solution was placed for another 6 h at room temperature. The resultant yellow precipitate was treated by filtering and rinsing with distilled water. The precursor ($Mo((C_2H_5)_2NCS_2)_2O_2$) was prepared by drying the product in vacuum at 60 °C for 12 h. Next, 0.5 g $Mo((C_2H_5)_2NCS_2)_2O_2$ was dissolved in 32 mL of distilled water, and the solution was then transferred to a 40 mL of Teflon-lined stainless steel autoclave. The autoclaves were heated at 200 °C for 12 h, and then allowed to cooled to room temperature. The resulting precipitates were finally obtained by filtering and washing with distilled water and ethanol, and drying at 80 ºC.

### Fabrication of the electrochemical glucose sensor

The bare GCEs were firstly treated by polishing using 0.3 and 0.05 μm alumina slurry and then rinsing with distilled water. The GCEs were then sonicated in a 1:1 nitric acid-water (v/v) solution, acetone and distilled water, and naturally dried at room temperature. 2.0 mg of $MoS_2$ materials were ultrasonically dispersed into 1.0 mL of 0.5% chitosan solution. Next, 1.0 mg of GOx powder was mixed evenly with 100 μL of the $MoS_2$-chitosan solution under stirring for 15 min at a slow speed. The mixed solution (5.0 μL) was casted on the pre-treated GCEs, and dried at 4 ºC in a refrigerator. The GOx/$MoS_2$/chitosan modified GCEs were finally rinsed with distilled water to remove unfixed enzyme molecules. When not in use, the enzyme electrodes were stored in a 0.1 M PBS (pH=7.0) at 4 ºC.

## Results and discussion

### Characterizations of nanorod-like $MoS_2$, $MoS_2$/chitosan and GOx/$MoS_2$/chitosan/GCE

Scanning electron microscopy was used to characterize the nanorod-like $MoS_2$ nanostructure and GOx loaded in the $MoS_2$/chitosan film. Fig.1A shows the SEM image of $MoS_2$ nanostructure, and a nanorod-like nanostructured morphology was observed clearly. Fig.1B shows the SEM image of the $MoS_2$/chitosan film. It can be seen that nanorod-like $MoS_2$ is dispersed in chitosan film. Fig.1C shows the SEM image of GOx/$MoS_2$/chitosan film. As seem from the SEM, a layer of aggregated enzyme was uniformly trapped into the $MoS_2$/chitosan film, indicating the successful fabrication the $MoS_2$-based glucose biosensor.

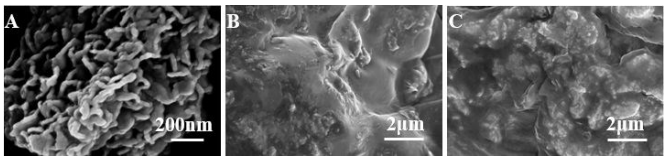


**Fig. 1** SEM images of nanorod-like $MoS_2$ (A), $MoS_2$/chitosan (B), GOx loaded in $MoS_2$/chitosan (C).

Electrochemical impedance spectroscopy was explored to investigate the modification process for the enzyme electrode. The semicircle part in Nyquist plot is ascribed to the electron-transfer limited process and its diameter depicts the electron transfer resistance (*R*ct). Fig. 2A displays the Nyquist plots of the pretreated GCE, and chitosan, $MoS_2$/chitosan, and GOx/$MoS_2$/chitosan modified GCEs, which was conducted within a frequency range of 0.05 to 10 kHz. The pretreated GCE has a very small *R*ct (15 Ω). When chitosan and $MoS_2$/chitosan were modified on the GCE, the *R*ct values of chitosan/GCE (55 Ω) and $MoS_2$/chitosan/GCE (84 Ω)



 

View Article Online
DOI: 10.1039/D0AN01557A



obviously increased. Moreover, the *R*ct value of $MoS_2$/chitosan/GCE is bigger compared with chitosan/GCE, suggesting that successful modification of $MoS_2$/chitosan film on GCE surface. After the GOx/$MoS_2$/chitosan was coated on the GCE, the *R*ct value (172 Ω) of GOx/$MoS_2$/chitosan/GCE greatly increased, suggesting the successful capture of enzyme on the modified electrode surface.

FT-IR spectroscopy was explored to examine the condition of the loaded GOx on modified electrode. FT-IR spectra of $MoS_2$ (curve a), $MoS_2$/chitosan (curve b), native GOx (curve c), and GOx/$MoS_2$/chitosan (curve d) were shown in Fig. 2B. FT-IR spectrum of $MoS_2$/chitosan shows two characteristic adsorption peaks at 1068 and 1403 $cm^{-1}$, which were ascribed to frame symmetric and asymmetric flexible vibrations and $CH_2$ bending vibration, respectively. As seen from FT-IR spectrum of singe GOx, two characteristic absorption peaks corresponding to amides I and II of GOx can be seen at 1611 and 1543 $cm^{-1}$. It was found that GOx/$MoS_2$/chitosan also displays two clear peaks at 1638 and 1551 $cm^{-1}$, corresponding to characteristic absorption of amide I and II bands of GOx molecules. This indicates that GOx has been successfully trapped in the composite film and maintains its biological activity. The slight shift of peak positions may be the absorption action of the GOx and the $MoS_2$/chitosan composite.

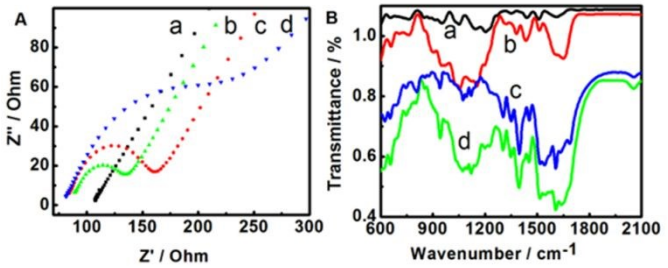


**Fig. 2.** (A) EIS from the pretreated GCE (a), chitosan/GCE (b), $MoS_2$/chitosan/GCE (c), and GOx/$MoS_2$/chitosan/GCE (d); (B) FTIR spectra of $MoS_2$ (a), $MoS_2$/chitosan (b), GOx (c), and GOx/$MoS_2$/chitosan (d).

**Direct electrochemistry action of GOx/$MoS_2$/chitosan modified electrode**

The DET behavior of GOx/$MoS_2$/chitosan/GCE was tested using cyclic voltammetry in 0.1 M $N_2$-saturated PBS at a scan rate of 100 mV $s^{-1}$. The cyclic voltammograms (CVs) of various modified electrodes were observed from Fig. 3. No redox peaks were seen at bare GCE (a) and $MoS_2$/chitosan/GCE (b). In comparison with bare GCE and $MoS_2$/chitosan/GCE, GOx/chitosan/GCE shows a pair of weak redox peaks at -0.422 and -0.476 V. It is worth mentioning that GOx/$MoS_2$/chitosan/GCE demonstrates a couple of intense and well-defined redox peaks at almost same potential. And the reduction peak current of GOx/$MoS_2$/chitosan modified GCE is 3.35 times larger than that of GOx/chitosan modified GCE, indicating that $MoS_2$ nanostructure greatly enhanced the electrical contact between redox-active center of GOx and the modified electrode surface. Thus the direct electron transfer between GOx and modified electrode was promoted. The peak potential difference of GOx/$MoS_2$/chitosan is 54 mV, which is much smaller than the value of 80 mV at GOx/graphene-chitosan/GCE[31], indicating rapid DET of GOx on $MoS_2$ modified electrode.

Fig. S1A reveals the cyclic voltammetry response of GOx/$MoS_2$/chitosan/GCE under different scan speeds. As the scan speed changed from 10 to 200 mV $s^{-1}$, the currents of the anode ($I_{pa}$) and cathode ($I_{pc}$) peaks increased linearly, and the

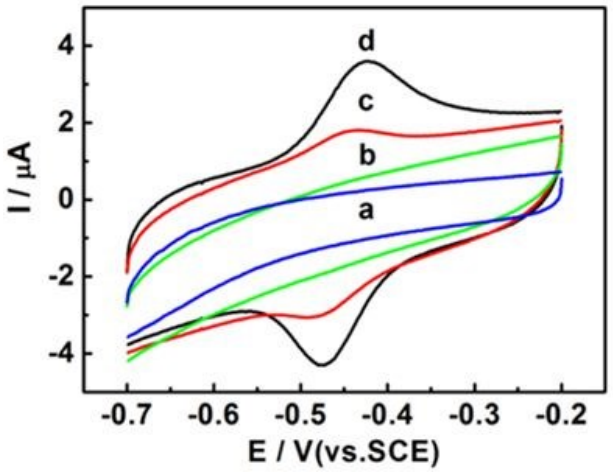


**Fig. 3.** CVs of bare GCE (a), $MoS_2$/chitosan/GCE (b), GOx/chitosan/GCE (c), and GOx/$MoS_2$/chitosan/GCE (d) performed in 0.1 M of $N_2$-saturated PBS (pH=7.0) with a scan speed of 100 mV $s^{-1}$.

redox potential of the electrode shifted slightly. In addition, the ratio of the $I_{pa}/I_{pc}$ is approximately 1.0, suggesting that the DET of GOx at the $MoS_2$ modified GCE belongs to a quasi-reversible surface controlled process. As seen from Fig. S1 A(II), the logarithm of the peak current of the cathode has a good linear relationship with the logarithm of the scan rate ($R^2$=0.9972), and the slope is 1.013, which is an approximation of theoretical slope of thin-layer electrochemistry. On the basis of Laviron's equation, the electron-transfer coefficient and electron transfer rate constant (κs) of the electrochemical sensor was 0.5 and 4.09 $s^{-1}$, respectively. The κs value of GOx/$MoS_2$/chitosan/GCE is larger than those of 2.85 $s^{-1}$ at GOx/PbS modified GCE[18], 3.68 $s^{-1}$ at GOx/$SnS_2$ modified GCE[22], and 2.83 $s^{-1}$ at GOx/graphene-chitosan modified GCE [31], further confirming that the nanorod-like $MoS_2$ can achieve the faster electron transfer of enzyme on the modified electrode. The surface coverage (Γ*) of the electroactive GOx on the $MoS_2$-modified electrode was calculated to be $3.74\times10^{-10}$ mol $cm^{-2}$, which is larger than $9.8\times10^{-12}$ mol $cm^{-2}$ of the GOx/Au modified carbon paste electrode[37], $1.60\times10^{-11}$ mol $cm^{-2}$ of GOx/$SnS_2$/Nafion/GCE[22] and $4.68\times10^{-11}$ mol $cm^{-2}$ of GOx/PbS/Nafion/GCE[18], indicating relatively large adsorption amount of enzyme on $MoS_2$ modified GCE.

Fig. S1B investigated the electrochemical behavior of GOx immobilized on $MoS_2$ modified electrode under different pH conditions. It was found that the potentials of anode and cathode peaks shifted negatively as the pH gradually increased from the range of 5.0-9.0. The formal potential of GOx/$MoS_2$/chitosan/GCE

View Article Online
DOI: 10.1039/D0AN01455A



changed linearly with the pH value of solution with a slope of -48.9 mV $pH^{-1}$ (shown in inset I of Fig. S1B). The value is close to the theoretical slope of -58.6 mV $pH^{-1}$, demonstrating that the electrochemical behavior is a same electron coupled same proton transfer process. As seen from inset II of Fig. S1B, the peak currents of anode and cathode get the maximum at a pH 7.0, indicating the suitable pH medium for the DET process.

**Detection mechanism and performance of the glucose biosensor**

The CVs of GOx/$MoS_2$/chitosan/GCE in $N_2$-saturated and air-saturated PBS containing different concentration of glucose were shown in Fig. 4A. The current of cathodic peak of GOx/$MoS_2$/chitosan/GCE displays a great increase in air-saturated PBS, which is ascribed to the increased account of GOx(FAD). The result indicates an electrocatalytic reduction reaction toward dissolved oxygen illustrated Eq (1) and (2). Once a certain amount of glucose was injected to the air-saturated PBS, the cathodic peak current of GOx/$MoS_2$/chitosan/GCE reduced gradually. This is because that the enzyme catalytic reaction restricts the electrocatalytic process toward the reduction of dissolved oxygen, resulting in the decrease of GOx (FAD) according to Eq (3). As a contrast, cyclic voltammograms of $MoS_2$/chitosan/GCE was also studied under same condition (Fig. 4B). No redox peak was observed in air-saturated PBS, but its reduction current enhanced greatly at more negative potential. However, no obvious change in reduction current was seen after injection of glucose to the air-saturated PBS. These results confirm that the electrochemical glucose can be explored for quantitative detection of glucose base on DET process toward GOx on $MoS_2$/chitosan/GCE.

$$GOx(FAD) + 2e^- + 2H^+ \leftrightarrow GOx\ (FADH_2) \quad (1)$$

$$GOx\ (FADH_2) + O_2 \rightarrow GOx\ (FAD) + H_2O_2 \quad (2)$$

$$GOx(FAD)+Glucose+O_2 \leftrightarrow GOx(FADH_2) + Gluconolactone \quad (3)$$

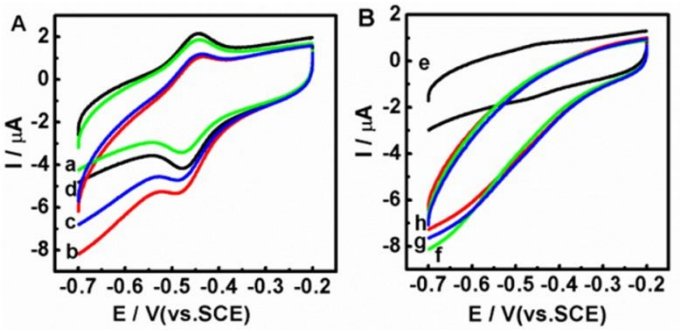


**Fig. 4.** CVs of GOx/$MoS_2$/chitosan modified GCE (A) and $MoS_2$/chitosan modified GCE (B) in 0.1 M of $N_2$-saturated PBS (a and e), air-saturated PBS (b and f), air-saturated PBS including 0.5 mM of glucose (c and g) and 0.1 mM of glucose (d and h) at a scan rate of 100 mV $s^{-1}$.

Fig. 5 shows the amperometric response on GOx/$MoS_2$/chitosan/GCE with continuous addition of glucose to air-saturated PBS system. To obtain optimal determination of glucose, reduction potential and pH value were chosen at -0.45 V and 7.0, respectively. The steady-state current response of the GOx/$MoS_2$/chitosan/GCE was less than 8 s. As shown in insets I and II of Fig. 5, the amperometric response currents were linearly related to glucose concentration from $1.5\times10^{-5}$ to $3.25\times10^{-4}$ M and $3.25\times10^{-4}$ to $1.43\times10^{-3}$ M with a low detection limit of $5\times10^{-6}$ (S/N=3), and the linear regression equations were I /μA = 2.4476 [glucose] / mM -3.6975 ($R^2$ = 0.9997) and I /μA = 1.6583 [glucose] / mM -3.3851 ($R^2$ = 0.9994). The sensitivity of the glucose sensor was calculated to be 25.06 ± 0.5 mA $M^{-1}$ $cm^{-2}$. Table S1 demonstrated a comparison between this glucose biosensor and others previous glucose biosensors reported in recent literature. It was found that the sensitivity of $MoS_2$-based glucose biosensor was superior to other material-based biosensors. The satisfactory performance

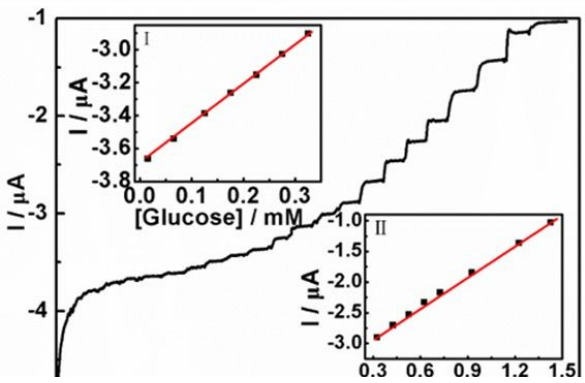


**Fig. 5.** The time-current curve of GOx/$MoS_2$/chitosan modified GCE by the successive addition of glucose into 0.1 M of air-saturated PBS at an applied potential of -0.45 V, insets I and II: plots of current vs. glucose concentration.

of the present electrochemical sensor is ascribed to the special structure and large specific surface area of $MoS_2$ semiconductor material.

**Interference, reproducibility and stability studies**

Fig. 6 shows the interference study of the $MoS_2$-based biosensor for glucose determination at an applied potential of -0.45 V. When adding 0.2 mM of glucose to PBS system, the biosensor displays a large current response. Then 0.1 mM of ascorbic acid (AA), 0.1 mM of uric acid (UA) and 0.1 mM of dopamine (DA) were successively added to the system, and no clear current responses were observed. When addition of another 0.2 mM glucose, an almost same current response appeared again. The results show that the $MoS_2$-based electrochemical biosensor demonstrates a good selectivity toward glucose in the presence of interfering substances. The fabrication reproducibility of the enzyme biosensor was investigated by determining 0.05 mM of glucose using five batches of glucose biosensor. The relative standard deviation (RSD) for the five measurements was 3.24%. The measurement of 0.05 mM of glucose for five times was used to examine the detection reproducibility of the biosensor, and the RSD was 1.66%. The results indicate the excellent reproducibility of the $MoS_2$-based electrochemical biosensor. The enzyme biosensor was stored in 0.1 M of PBS (pH=7.0) at 4 °C in a refrigerator when not in use. The glucose biosensor still maintained 96% of the initial current response after 21 days of storage, indicating the biosensor has acceptable stability.

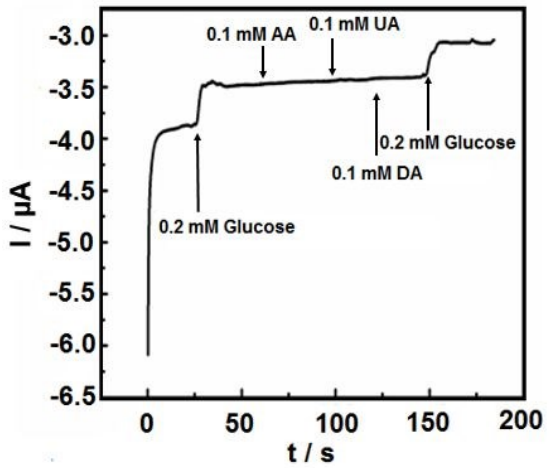


**Fig. 6.** Amperometric curve of GOx/$MoS_2$/chitosan modified GCE toward 0.2 mM of glucose, 0.1 mM of AA, 0.1 mM of UA and 0.1 mM of DA in 0.1 mM of PBS (pH=7.0) at an applied potential of -0.45 V.

**Detection of practical samples**

In order to evaluate the practicality of the glucose sensor, human serum samples were measured using the GOx/$MoS_2$/chitosan/GCE. The serum samples were friendly provided by Northern Jiangsu People's Hospital. The samples need no pre-treatment process except a dilution step. The glucose concentration in a serum sample was measured to be 5.15 mM by the present biosensor, which is close to 5.32 mM measured by the local hospital. Next, the recovery experiments were carried out by the addition of 0.1mM, 0.2 mM and 0.3 mM standard glucose to the serum sample, respectively, and the detection results were shown in table 1. The recoveries of the samples were 107.0%, 101.5% and 97.03%, respectively. The results show that the electrochemical biosensor can be successfully used in the detection of practical serum samples.

**Table 1** Recovery for detection of glucose in human serum samples

| Sample | Added ( mM ) | Found ( μM ) | Recovery ( %, *n*=5 ) | RSD ( % ) |
|---|---|---|---|---|
| 1 | 0.100 | 0.107 | 107.0 | 0.46 |
| 2 | 0.200 | 0.203 | 101.5 | 0.35 |
| 3 | 0.300 | 0.291 | 97.03 | 1.08 |

## Conclusions

In summary, we reported the synthesis of a nanorod-like $MoS_2$ nanostructure to trap enzymes and electrochemical biosensing of glucose based DET of GOx molecules. The nanorod-like $MoS_2$ nanostructure, which was characterized with various testing methods, shows provides a special structure and large specific surface area for GOx immobilization. GOx on the $MoS_2$ nanostructure retained the native structure and high bioactivity, and the DET of enzyme loaded on the modified electrode was accelerated greatly. Therefore, the electrochemical glucose biosensor shows excellent performance such as high sensitivity, good selectivity, acceptable reproducibility and stability. Moreover, human serum samples were measured with the present biosensor, showing the good practical capability in the detection of real samples. This research offered a potential electrode material for electrochemical biosensing applications.

## Conflicts of interest

There are no conflicts to declare.

## Acknowledgements

The authors will acknowledge the financial support by National Natural Science Foundation of China (21575125, 21575124 and 21475116), Natural Science Foundation of Jiangsu Province (BK20191434), 333 Project and Qinglan Project of Jiangsu Province, and High-end talent support program of Yangzhou University for Zhanjun Yang, and Juan Li, Priority Academic Program Development of Jiangsu Higher Education Institution (PAPD), Six Talent Peaks Project of Jiangsu Province for Zhanjun Yang and Juan Li, Open Research Fund of State Key Laboratory of Analytical Chemistry for Life Science (no. SKLACLS1915).

## Notes and references

1 F.F. Zhang, Q. Wan, X.L. Wang, Z.D. Sun, Z.Q. Zhu, Y.Z. Xian, L.T. Jin, K. Yamamoto, *J. Electroanal. Chem.*, 2004, **571**, 133-138.
2 S.N. Sarangi, S. Nozaki, S.N. Sahu, *J. Biomed. Nanotechnol.,* 2015, **11**, 988-996.
3 J. Wang, *Biosens. Bioelectron.*, 2006, **21**, 1887-1892.
4 R. Ahmad, N. Tripathy, M.-S. Ahn, K.S. Bhat, T. Mahmoudi, Y.S. Wang, J.-Y. Yoo, D.-W. Kwon, H.-Y. Yang, Y-B. Hahn, *Sci. Rep.*, 2017, **7**, 5715.
5 L.H. He, Q.B. Liu, S.J. Zhang, X.T. Zhang, C.L. Gong, H.H. Shu, G.J. Wang, H. Liu, S. Wen, B.Q. Zhang, *Electrochem. Commun.*, 2018, **94**, 18-22.
6 P. Gomathi, M. K. Kim, J. J. Park, D. Ragupathy, A. Rajendran, S. C. Lee, J. C. Kim, S. H. Lee, H.D. Ghim, *Sens. Actuators, B: Chem.*, 2011, **155**, 897-902.
7 H. Guan, D. Gong, Y. Song, B. L. Han, N. Zhang, *Colloids and Surf. A*, 2019, **574**, 260-267.
8 A. A. Karyakin, *Bioelectrochemistry*, 2012, **88**, 70-75.
9 J. Wang, *Chem. Rev.* 2008, **108**, 814-825.
10 J. Rajbongshi, D. K. Das, S. Mazumdar, *Electrochem. Acta* 2010, **55**, 4174-4179.
11 S. Zhao, K. Zhang, Y. Bai, W. W. Yang, C. Q. Sun, *Bioelectrochemistry*, 2006, **69**, 158-163.
12 J. J. Gooding, R. Wibowo, J. Q. Liu, W. Yang, D. Losic, S. Orbons, F. J. Mearns, J. G. Shapter, D. B. Hibbert, *J. Am. Chem. Soc.*, 2003, **125**, 9006-9007.
13 H. Behzad, A. T. Mahmoud, *Electrochem. Acta*, 2011, **56**, 10101-10106.
14 F. Jia, C. S. Shao, F. H. Li, L. Niu, *Biosens. Bioelectron.*, 2008, **24**, 951-956.
15 Y. Zhang, Q. Wei, *J. Electroanal. Chem.*, 2016, **781**, 401-409.
16 J. Li, Y. Liu, X. Tang, L. J. Xu, L. F. Min, Y. D. Xue, X. Y. Hu, Z. J. Yang, *Microchim. Acta*, 2020, **187**, 80.
17 J. Li, M. M. Lu, Z. N. Tan, Y. B. Xu, Y. C. Zhang, X. Y. Hu, Z. J. Yang, *Microchim. Acta*, 2016, **183**, 1705-1712.

View Article Online
DOI: 10.1039/D0AN01553A



18 J. Li, Y. Tang, J. Yang, Z. J. Yang, Y. C. Zhang, X. Y. Hu, *Sens. Actuators, B: Chem.*, 2014, **190**, 549-554.
19 Y. L. Wu, Q. W. Li, X. L. Zhang, X. Chen, X. M. Wang, *Chin. Chem. Lett.*, 2013, **24**, 1087-1090.
20 J. T. Luo, M. Xie, P. X. Luo, B. X. Zhao, K. Du, P. Fan, *Mater. Lett*., 2014, **130**, 14-16.
21 H. C. Kazici, M. Yalya, *Chem. Eng. Commun.*, 2019, **206**, 1731-1742.
22 Z. J. Yang, Y. Y. Ren, Y. C. Zhang, J. Li, H. B. Li, X. C. Huang, X. Y. Hu, Q. Xu, *Biosens. Bioelectron.*, 2011, **26**, 4337-4341.
23 W. Wei, J. P. Nong, L. L. Tang, N. Wang, C. J. Chuang, Y. Huang, *Plasmonics*, 2016, **12**, 1205-1212.
24 J. Wang, J. L. Liu, D. L. Chao, J. X. Yan, J. Y. Lin, Z. X. Shen, *Adv. Mater.*, 2014, **26**, 7162-7169.
25 S. Das, C. Kumar, R. Kumar, A. Srivastava, S. Jit, *IEEE Photon. Technol. Lett.*, 2020, **32**, 67-70.
26 C. Zeng, J. Pu, H. Wang, S. J. Zheng, L. P. Wang, Q. J. Xue, *Ceram. Int.*, 2019, **45**, 15834-15842.
27 H. J. Liang, P. Hua, Y. F. Zhou, Z. M. Fu, J. N. Tang, J. F. Niu, *Chin. Chem. Lett.*, 2019, **30**, 2245-2248.
28 S. Maulik, S. Basu, K. Kanakamedala, T. Daniels, *J. Electron. Mater.*, 2019, **48**, 3451-3458.
29 K. Chang, D. Geng, X. F. Li, J. L. Yang, Y. J. Tang, M. Cai, R. Y. Li, X. L. Sun, *Adv. Energy Mater.*, 2013, **3**, 839-844.
30 J. W. Zhou, J. Qin, N. Q. Zhao, C. S. Shi, E. Z. Liu, F. He, J. J. Li, C. N. He, *J. Mater. Chem. A*, 2016, **4**, 8734-8741.
31 J. Yoon, T. Lee, B. Bapurao G., J. Jo, B.-K. Oh, J.-W. Choi, *Biosens. Bioelectron.,* 2017, **93**, 14-20.
32 T.Y. Wang, R.Z. Zhu, J.Q. Zhuo, Z.W. Zhu, Y.H. Shao, M.X. Li, Anal. Chem. 2014, **86**, 12064-12069.
33 Y. Guo, Y. Shu, A. Li, B. Li, J. Pi, J. Cai, H. Cai, Q. Gao, J. Mater. Chem. B, 2017, **5**, 5532-5538.
34 W.J. He, Y.X. Huang, J. Wu, *Nano Res. Lett.* 2020, **15**, 60.
35 S. Su, Z. W. Lu, J. Li, Q. Hao, W. Liu, C. F. Zhu, X. Z. Shen, Z. Y. Shi, L. H. Wang, *New J. Chem.*, 2018, **42**, 6750-6755.
36 S. K. Shukla, S. R. Deshpande, S. K. Shukla, A. Tiwari, *Talanta*, 2012, **99**, 283-287.
37 L. M. Liu, J. W. Wen, L. J. Liu, D. Y. He, R. Y. Kuang, T. Q. Shi, *Anal. Biochem.*, 2013, **445**, 24-29.

View Article Online
DOI: 10.1039/D0AN01553A



Graphical Abstract:

**Facile synthesis of nanorod-like $MoS_2$ nanostructure for sensitive electrochemical biosensing application**

*By* Zhongfang Hu,[a] Rong Xu,[a] Suhua Yu,[b] Juan Li,[a,*] Zhanjun Yang[a,b]

A novel nanorod-like $MoS_2$ semiconductor nanostructure was synthesized through a simple two-step method, and then was exploited as electrode material to immobilized glucose oxidase (GOx) and electrochemical sensing application.